Comments on Inorganic Chemistry
Publication details, including instructions for authors and subscription information:
http://www.informaworld.com/smpp/title~content=t713455155

Biological Electron Transfer: The Structure, Dynamics and Reactivity of Cytochrome *c*

Glyn Williams[a]; Geoffrey R. Moore[a]; Robert J. P. Williams[a]
[a] Inorganic Chemistry Laboratory, University of Oxford, Oxford, United Kingdom

To cite this Article Williams, Glyn , Moore, Geoffrey R. and Williams, Robert J. P.(1985) 'Biological Electron Transfer: The Structure, Dynamics and Reactivity of Cytochrome *c*', Comments on Inorganic Chemistry, 4: 2, 55 — 98
To link to this Article: DOI: 10.1080/02603598508072253
URL: http://dx.doi.org/10.1080/02603598508072253

Biological Electron Transfer: The Structure, Dynamics and Reactivity of Cytochrome *c*

1. INTRODUCTION

Cytochrome *c* is the best characterized member of a group of over 50 metallo- and flavo-proteins which constitute the mitochondrial respiratory electron transport chain. It is a comparatively small (103–111 amino acid residues), stable, water-soluble protein containing a single haem prosthetic group which cycles between the Fe(II) and Fe(III) states in the course of its electron transfer reactions. In a recent Faraday Society Discussion we presented a paper[1] which concluded with the following paragraphs:

> Is cytochrome *c* an ideal electron-transfer reagent? The suggestion has frequently been made that biological systems have found by random searching almost perfect solutions to chemical problems. The observation of constant redox potential of many different mitochondrial cytochromes *c* from very different species, and the similarities in electron self-exchange rate constants, support this argument. It appears as if mitochondria have "homed in" on these properties despite sequence variations.
>
> Many of the requirements for fast electron transfer are known. The redox potential is one such control. A second is the ability of the coordination sphere to relax. Phe82 is mobile and the Fe(III)–S bond is adjustable, perhaps all the surrounding protein at the haem edge is adjustable. Good relaxation conditions are therefore met. The distance between redox centres within complexes of ca. 1–2 nm is long, but it may well be the optimum since two recognition surfaces are required between the centres. Thus given the requirements of biological systems, especially of self-assembly, cytochrome *c* may well be close to being an ideal electron transfer reagent.

Comments Inorg. Chem.
1985, Vol. 4, No. 2, pp. 55–98
0260-3594/85/0402-0055/$30.00/0

In this Comment we shall consider some of these points again in the light of our most recent work. The aim of the work is to characterize the structure and dynamics of cytochrome *c* and in particular to identify redox-dependent changes in the protein, but we preface this with some general remarks on the electron-transfer reaction and the nature of protein structures. We hope that these opening remarks and the subsequent description of cytochrome *c*, the first protein for which detailed information about solution structure and dynamics is available, will help the inorganic chemist to see how complicated an object a metalloprotein is, and to recognize the parallels between the effects of the protein on haem reactivity and the effects of solvent on simpler chemical systems. Although we concentrate on cytochrome *c* our approach and conclusions are generally applicable to all classes of electron-transfer proteins.[2]

2. ELECTRON-TRANSFER REACTIONS OF CYTOCHROME *c*

The outer-sphere electron-transfer reactions between small metal ion complexes have been extensively investigated from the standpoint of Marcus theory.[3-5] A five-step mechanism is envisaged in which the reactants first diffuse together:

$$A^- + B \rightleftarrows (A^- \cdot B) \tag{1}$$

This is followed by some structural reorganization of the bond lengths and angles of the complex and the surrounding solvent in order that the electron transfer step may occur isoenergetically.

$$(A^- \cdot B) \rightleftarrows \{A^- \cdot B\} \tag{2}$$

$$\{A^- \cdot B\} \rightleftarrows \{A \cdot B^-\} \tag{3}$$

Subsequent relaxation yields the equilibrium configuration of the product complex and is followed by diffusion apart to give the separated products

$$\{A \cdot B^-\} \rightleftarrows [A \cdot B^-] \tag{4}$$

$$[A \cdot B^-] \rightleftarrows A + B^- \qquad (5)$$

Steps (2), (3) and (4) are represented schematically in Fig. 1. The motion of the electron satisfies the Franck–Condon principle that electronic and nuclear motions are not coupled and the mechanism has elements in common with both transition-state theory and the description of transitions in electronic spectra. The complex within which the electron is transferred (represented by curly brackets) has the property that its free energy is independent of the position of the electron, hence the electron may be transferred between the donor and acceptor centers without the absorption or emission of light. If the distortions of the reactant and product complexes that lead to the electron-transfer complex are assumed to be harmonic vibrations,

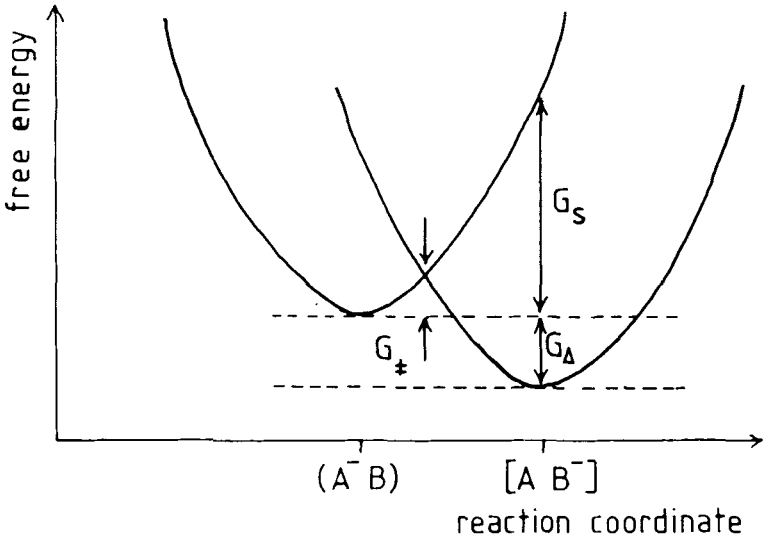

FIGURE 1 Marcus-theory description of the energetic changes leading to electron transfer *within* a reactive complex. The potential-energy surfaces formed by distortions of the reactant and product complexes are assumed to be parabolic and the activation free energy, $G_{\ddagger}$, is related to the redox driving energy, G_{Δ}, and the free energy required to transform the geometry of the reactant complex into that of the product complex without electron transfer, G_S, according to Eq. (6). Note that the redox driving energy may not be the same as the redox potential difference of the isolated species, although they are often assumed to be the same (Refs. 6 and 7).

the activation energy for the electron-transfer step, $G_{\neq}$ is related to the quantities G_{Δ} and G_S (Fig. 1) by the expression

$$G_{\neq} = (G_{\Delta} + G_S)^2/4G_S \tag{6}$$

The calculated second-order rate constant, k_{calc}, for the overall electron-transfer reaction is then given by

$$k_{calc} = K_d \nu \kappa \exp(-G_{\neq}/RT) \tag{7}$$

where K_d is the equilibrium constant for the pre-association step (1), ν is a pre-exponential factor describing the rate at which energy may be transferred along the reaction coordinate (approximately 10^{13} s^{-1} for a vibrationally activated process) and κ is a transmission coefficient which describes the probability of electron transfer once the appropriate geometry has been reached.

The same reaction scheme may be applied to the electron-transfer reactions of proteins such as cytochrome *c*. In such a system a wide range of vibrational and torsional modes are available, through which the energy of the electron at the acceptor and donor sites may be controlled. In addition, cytochrome *c* is asymmetric and may form a number of different complexes with the redox partner; thus we must consider the possibility that there is no longer a unique complex through which electron-transfer proceeds.

Despite the practical difficulties, a molecular description of the reactions of cytochrome *c* must include those structural alterations that affect the energy of the electron at the haem in the reactive complex. We make the simplifying assumption that these changes in cytochrome *c* do not depend on the precise nature of the redox partner. Both the extent of these changes and their effects on the haem redox potential are of importance. Thus a large movement of an amino acid side-chain far from the haem may not affect the haem potential directly but rather indirectly, through much smaller displacements of groups packed around the haem, or by movements of the haem group itself or its ligands, or via long-range electrostatic effects. In a haem-centered view it would be said that a change in the redox center of cytochrome *c* requires small alterations of side chains in the vicinity of the haem which are amplified towards the more mobile protein exterior. Although the protein is the "solvent"

for the haem it acts in a cooperative manner, and is more like a crystal lattice in this respect.

Using nuclear magnetic resonance spectroscopy (NMR) we have set out to investigate the structure and dynamics of both oxidation states of cytochrome *c* in solution. Although it is not yet possible to present a complete high-resolution structure of cytochrome *c* based on NMR data alone, several regions of the protein have been well defined and the major redox-dependent changes have been characterized. Before these results are summarized and their implications are discussed we must first clarify our view of protein structure in solution.

3. THE DYNAMIC NATURE OF PROTEIN STRUCTURES

A complete description of the structure of a protein requires that the position of each of its atoms be known as a function of time in the biochemically relevant environment. Such a description has not been achieved and it is difficult to see how it could be. Nevertheless, it is becoming customary to relate the chemical and biochemical properties of a protein to a static model of its structure as determined by crystallographic methods under nonphysiological conditions and then to refine this model by studies of structure and dynamics in solution.[8] Our description of the time-average structure of cytochrome *c* in solution is based upon just such a refinement of the crystallographic structure using NMR data as fitted parameters. However, because of their different time scales, the x-ray and NMR experiments usually observe different dynamic events. Thus a description of protein dynamics must rely on evidence from a large number of essentially independent sources.

Before discussing the dynamic behavior of cytochrome *c* we must clarify our interpretation of three quantities, namely frequency, amplitude, and rate. The frequency (ν) of a harmonic vibration depends on the force constant (C) and the reduced mass (μ) of the system such that

$$\nu = \sqrt{C/\mu} \tag{8}$$

The amplitude of any such motion is determined by the amount of energy stored in each quantized vibrational mode. The oscillation

occurs about a potential energy minimum and for atomic vibrations ν lies in the range 10^{10}–10^{14} s^{-1}.

Where motion can lead to a number of distinguishable structures their interconversion must be described as a rate process. For example, the rotation of an aromatic ring leads to the exchange of its two ortho protons with each other, and also of its meta protons with each other. Although the two rotamers are crystallographically indistinguishable, in the asymmetric environment of the protein interior their rate of exchange (k) can be measured by NMR and is given approximately by an Arrhenius expression:

$$k = \nu \exp\left(\frac{\Delta S}{R}\right) \exp\left(\frac{-\Delta E}{RT}\right) \tag{9}$$

where ν is the vibrational frequency of the torsional oscillation and ΔE is an activation energy. This is illustrated in Fig. 2. At any time only a limited number of molecules of the Boltzmann distribution

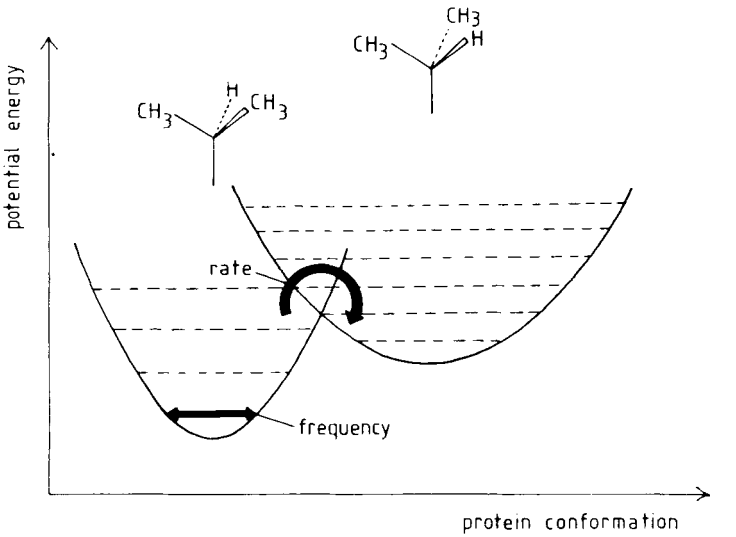

FIGURE 2 Rate processes and vibrational frequencies within a protein. Their distinction is illustrated using a valine residue which may exist in one of three conformations within the protein (two are illustrated). Interconversion between different conformations must be described as a rate process and each conformation will undergo torsional oscillations of characteristic frequency about a potential minimum.

possess an energy greater than or equal to ΔE in this vibrational mode. A molecule with less energy than ΔE must undergo collision with the solvent or with other molecules in order to gain energy and undergo reaction.

NMR measures *rate* processes, e.g., the flipping of a tyrosine ring or the stepwise rotation of a valine side-chain, but does not provide information on the *frequencies* or amplitudes of the oscillations in the energy wells which underlie these rate processes. In contrast, an analysis of the atomic B factors obtained from x-ray crystallography provides information on the amplitudes and, in principle, the frequencies of atomic displacements, provided all contributions from static disorder in the crystal can first be accounted for, but can supply no information on the *rates* of processes which lead to crystallographically indistinguishable structures (e.g., ring-flips). Where rate processes lead to nonidentical structures, e.g., valine rotation, it is difficult to distinguish in the electron density map between visits to multiple potential energy wells of a high frequency vibration and a low frequency vibration of large amplitude.

In the case of cytochrome *c*, electron transfer will occur from a limited number of vibrational states of a given conformation. If these states are populated vibrational states of the ground-state structure, the electron transfer will have no activation energy and the rate will represent a pure tunneling rate. However this may not be the case for the reactions of interest and we must consider the likely alternative that electron transfer occurs from excited vibrational levels of a non-ground-state conformation. As discussed in Section 2, the electron transfer will now require an energy of activation associated with the prior rearrangement of nuclear positions, and with the vibrational activation of that particular conformation. The electron-transfer rate is still related to a tunneling rate (which is itself dependent on the geometry of the chosen conformation and the degree of vibrational activation required) but is now limited by an additional Boltzmann term. In the case of proteins, such conformational activation may require changes in rotamer populations of asymmetric topped amino acid side-chains, or gross changes in the conformation of the polypeptide backbone. However, in order to participate, such changes *must* occur on a time scale equal to or shorter than the overall electron-transfer rate ($\sim 10^2$–$10^4\ s^{-1}$ for cytochrome *c*). Some dynamic events, their approximate time scales, and the experimental methods appropriate to their study are given in Table I.

TABLE I
Dynamic events internal to proteins

Dynamic Event	Time Scale (s)	Description	Method[8]*
(a) Vibration/Rotation	10^{-10} to 10^{-14}	Vibrations of small groups in single potential energy wells and rotations of small symmetric tops., e.g., methyl groups	x-ray diffraction (B-factor analysis) Molecular dynamics (theoretical analysis)
(b) Ring Flips	$> 10^{-10}$	Rotation of aromatic side-chain between degenerate conformations. If rapid, may show locally high B-factors or involve residues on the protein surface. If slow, may require rare events, e.g., conformational changes	NMR (line shape analysis and saturation transfer) Molecular mechanics
(c) Valine/Leucine Rotation	$> 10^{-10}$	Rotation of aliphatic side-chains (asymmetric tops) between nondegenerate conformations. For additional comments see (b)	x-ray diffraction (disorder analysis) NMR (chemical shifts, NOE's and coupling constant analysis)
(d) Conformational Segmental Motion (except termini)	$> 10^{-4}$	Conformational changes of polypeptide backbone	x-ray diffraction (absence of electron density) NMR (^{13}C relaxation time, H/D exchange)
(e) Protein Unfolding	$> 10^{-2}$	Gross cooperative conformational changes	NMR (H/D exchange) Circular dichroism, Fluorescence

*These methods do not usually measure both frequency and amplitude but only one of these quantities.

4. STRUCTURE DETERMINATION BY X-RAY CRYSTALLOGRAPHY AND NMR SPECTROSCOPY

As discussed above, an understanding of protein design and function requires knowledge of the energies and geometries of the dynamic states available to the structure. In the case of cytochrome *c* however, we can immediately exclude those structural changes such as ligand exchange and protein unfolding which occur on time scales longer than the electron-transfer reaction. These dynamic processes cannot be coupled to the activation process. At the other extreme, it is unlikely that changes in the rotational states of methyl groups, which rotate about their adjacent carbon–carbon bonds with time constants of about 10^{-12} s, can be coupled to the vibronic activation of the protein matrix.

The motions with which we are concerned consist of bond vibrations and the rotation or libration of sterically hindered amino acid side-chains and the polypeptide backbone, and result in cooperative changes throughout the protein structure. These motions include the "flipping" of aromatic rings between equivalent conformations and segmental motions of the polypeptide backbone. It is not our principal concern whether the motion involves visits to many different energy minima or to just two, but in order to be relevant the activation energy of the motion should be $\leqslant 20$ kT. It is against this background of structural dynamics that the information content of x-ray crystallography and NMR spectroscopy must be judged.

X-ray diffraction is the best general method for protein structure determination, partly because it is the only method to give an overall, detailed view of proteins. However, unlike x-ray diffraction studies of small molecules, the method is generally based upon model-building which can give a false impression of the structure at the atomic level. Fortunately, low-resolution structures (not at atomic resolution) often yield significant biochemical information, such as the symmetry of quartenary structure and approximate packing of subunits, the location and type of cofactors, the position and nature of secondary structure elements, and the approximate distribution of many amino acid side-chains. However, it is only at atomic resolution that structure-function relationships can be properly defined and at this resolution x-ray structures may be misleading, not only because of distortions caused by crystal packing and high salt concentrations, but also because, generally, x-ray structures are presented as a fitted,

static set of coordinates. It is important to realize that proteins cannot have a structure in the same sense that a sodium chloride lattice or a benzene lattice has a structure. There is considerable thermal motion throughout the protein that is composed mainly of side-chain movements, often with smaller main-chain movements, that are at a maximum at the protein surface. These motions are very rapid, with frequencies $> 10^9\ s^{-1}$. The dynamic processes are difficult to describe but generally their presence may be inferred from the quality of the x-ray electron-density images and from the study of thermal B-factors. However, mobility is often difficult to separate from static disorder. The fact that the x-ray experiment is done in a crystal lattice may lead to dampened segmental motion and enforced occupancy of a distorted structure.

NMR spectroscopy is not a general method for protein structure determination although considerable detail may be derived for small proteins which are relatively rigid. Its main strength is that it allows local regions of the structure to be investigated at high resolution under conditions approaching those of the physiological state. Also, NMR detects mobility over a wide time scale range much more easily than x-ray crystallographic methods and in many cases it gives rate constants for the mobility directly. Its main weakness lies in the difficulty with which dynamically averaged NMR parameters such as chemical shifts, relaxation rates, and coupling constants are translated into limiting structures for the motion.

Current work is directed towards allowing the crystallographic and spectroscopic techniques to interact. Theoretical calculations are of great help in understanding these problems. In a subsequent section of this Comment we describe briefly a calculation of the refinement of the orientation of the electronic *g*-tensor of ferricytochrome *c* which was performed using NMR chemical shift data in conjunction with the available x-ray coordinates. In the future we will use molecular graphics, energy minimization and molecular dynamics calculations to modify the crystal structure of cytochrome *c* in accordance with the NMR data, and to model the structural changes on oxidation or reduction in solution. Using these methods it is expected that cooperative changes in structures whose amplitudes are too small to be detected at present by NMR or x-ray diffraction, yet which contribute significantly to the vibronic activation of cytochrome *c*, may be determined. These deductions will eventually be subject to ex-

perimental test via chemical modification of the structure or site-directed mutagenesis (single amino acid replacements).

5. MITOCHONDRIAL CYTOCHROME *c* STRUCTURES

Seven independent x-ray structures have been determined[9–13] for various mitochondrial cytochromes *c* including structures of both redox forms, ferrocytochrome *c* and ferricytochrome *c*, and structures of proteins from different sources. Table II summarizes some of the relevant crystallographic information.

Although there is a relatively high level of agreement between the different structures, there are significant differences between some of them. These structural differences arise from three main effects: crystallographic distortions, the redox state difference and amino acid sequence differences. Each of these effects can be analyzed in detail by comparison of the relevant x-ray structures, both with each other and with solution NMR data, and although a full description of the results is beyond the scope of this Comment we shall consider some

TABLE II
X-ray crystal structures of cytochromes *c*

Protein	Space Group	Mol.[i]	Res.[ii]	Crystallization Solution	Ref.
Tuna Fe(III)	$P4_3$	2	1.8	7–11% cytochrome, 1.0 M ammonium phosphate (*p*H 7), 15% $NaNO_3$, 45–50% $(NH_4)_2SO_4$	12
Tuna Fe(II)	$P2_12_12$	1	1.5	10% cytochrome (*p*H 7.5), 85% $(NH_4)_2SO_4$	12
Horse Fe(III)	$P4_3$	1	2.8	? % cytochrome, 0.5–1.0 M NaCl (*p*H 6–7), 90–95% $(NH_4)_2SO_4$.	9,14
Bonito Fe(III)	$P2_12_12_1$	1	2.8	1–3% cytochrome, 0.05 M ammonium phosphate (*p*H 6), 83% $(NH_4)_2SO_4$.	11,15
Bonito Fe(II)	$P2_12_12_1$	1	2.3	7% cytochrome (*p*H 8), 60% $(NH_4)_2SO_4$	10,15,16
Rice Fe(III)	$P6_1$	1	2.0	2% cytochrome (*p*H 6), 3.6 M $(NH_4)_2SO_4$.	13

[i]Number of molecules; the two tuna Fe(III) structures are called "inner" and "outer."
[ii]Resolution (Å)

of these effects after a general description of the structural features common to all. We are of the opinion that the properties of biological interest of such proteins as cytochrome *c* can only be understood by detailed examination of *the whole structure,* since proteins are co-operative molecules. In this Comment we hope to demonstrate the need for this approach.

A. General Features of the Structure

The polypeptide chain is organized into five α-helical segments that contain ~45% of the amino acids (Fig. 3). There is no regular β-

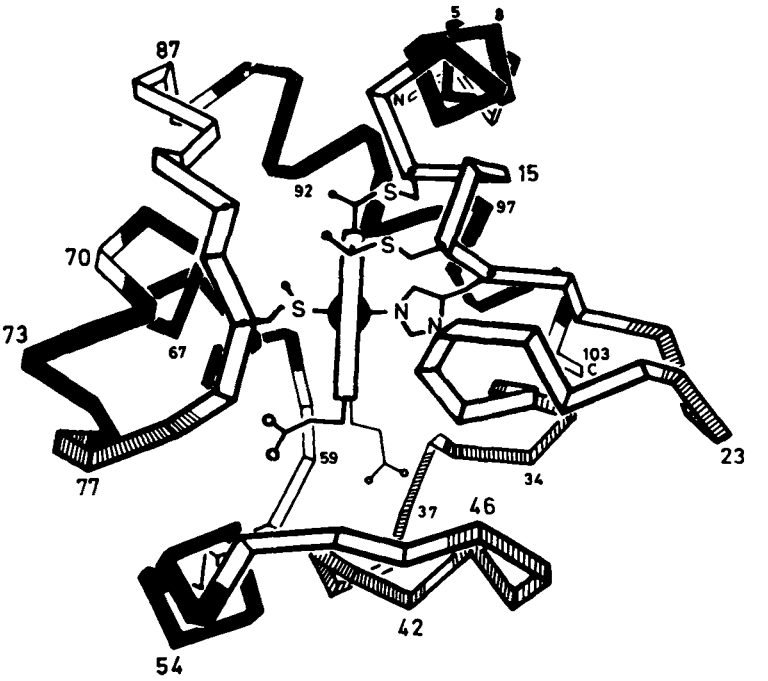

FIGURE 3 Ribbon diagram of tuna cytochrome *c* showing the polypeptide fold and haem orientation. This is the conventional view of cytochrome *c*; the protein is viewed looking onto the face bearing the exposed haem edge. Top, bottom, right, left, front and back refer to this orientation. α-helices are indicated by solid ribbons and type II 3_{10} bends by striped ribbons. The five α-helical stretches are: 3–12, 50–55, 61–69, 70–75 and 88–101. The six type II 3_{10} bends are: 21–24, 32–35, 35–38, 39–42, 43–46 and 75–78. The 39–42 bend is slightly deformed.

strand structure but there are six type II 3_{10} bends, most of which are located at the base and right-hand side of the structure according to the orientation of Fig. 3.

Amino acids have been classified into three groups according to the degree of exposure of their side-chains to the solvent[17]: exposed, partly exposed and buried (Fig. 4). Naturally, most of the charged residues are exposed and most of the hydrophobic residues are buried but the full significance of these groupings can only be appreciated by considering the way in which the haem and polypeptide interact.

The polypeptide chain wraps itself around the haem (Fig. 3) so that only a small part of the haem is exposed at the molecular surface: ~4% of the haem which forms ~0.06% of the molecular surface.[18] Covalent bonds between the haem and four amino acids—Cys14, Cys17, His18 and Met80—anchor the haem. Together with the extensive array of noncovalent side-chain contacts (Fig. 4 and Table III), these bonds help to make the internal structure relatively rigid. One of the striking features of this structure is that the propionic acid bearing edge of the haem is buried within the protein, completely shielded from the bulk solvent. This part of the internal structure is less rigid than the regions surrounding the haem macrocycle.

The analysis of protein function requires knowledge of the protein structure in solution under physiological conditions. By comparing NMR data from solutions with theoretical calculations based on the crystal structures we may identify similarities and differences between the solid state and solution in both the overall structure (the protein fold) and the local conformations of some amino acid side-chains, and we can begin to identify those regions of the protein which have unusual dynamic properties. This is necessary since the activity of any protein involves dynamic processes and changes of structure. The relationship we seek to understand is:

$$\text{sequence} \rightarrow \text{structure} \rightarrow \text{dynamics} \rightarrow \text{function}$$

B. The Structure of Cytochrome *c* in Solution

(i) The Pseudocontact Shift as a Structural Tool. In order to describe the overall structure in solution and the local conformations of the haem-packing residues (Fig. 4) we shall use the low-spin Fe(III) ion of ferricytochrome *c* as a rhombic NMR shift probe. In this procedure the electron–nucleus dipolar (pseudocontact) shift is calulated using

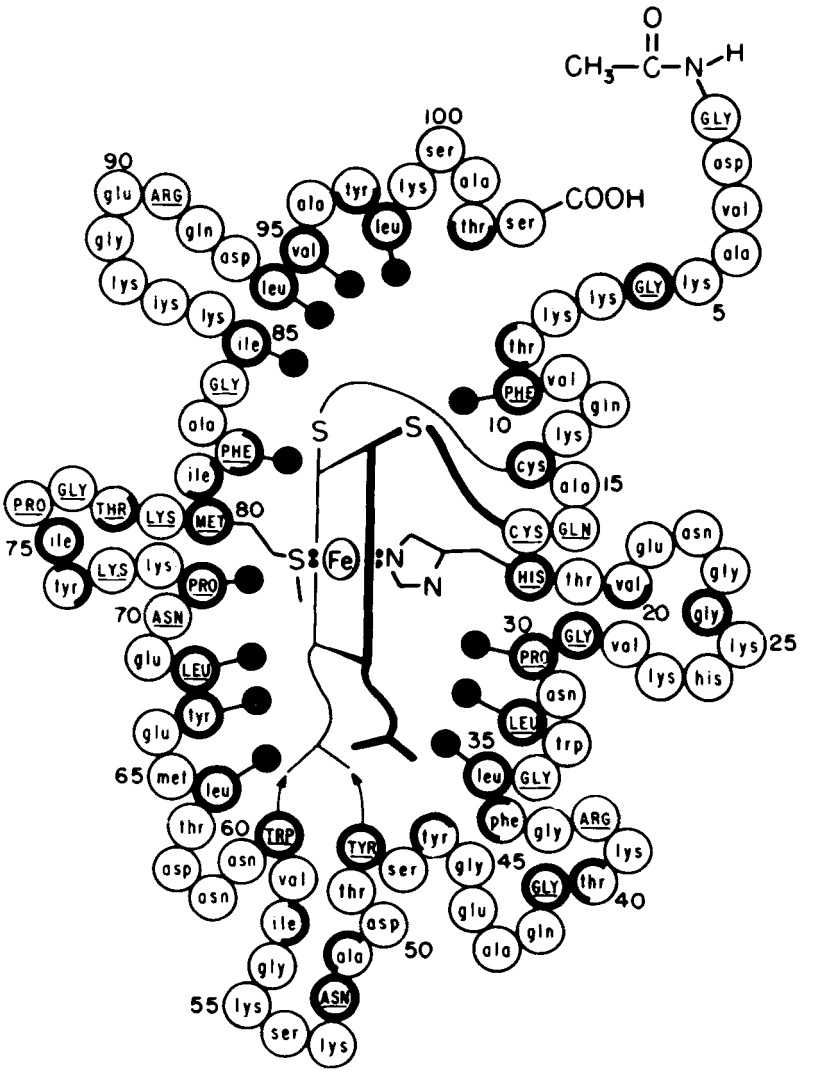

FIGURE 4 Chain packing diagram of tuna cytochrome *c* illustrating the classification of side-chains into buried (heavy circles), partially buried (heavy semicircles) and exposed (light circles) categories. Side-chains packed against the haem macrocycle are indicated by heavy black dots and invariant residues are underlined and upper case (adapted from Ref. 17).

TABLE III
Haem propionate interactions

Substituent 6 (HP-6)	Substituent 7 (HP-7)
Thr49N	Arg38
Thr49	Gly41N
Asn52	Tyr48
Thr78	Asn52
	Trp59
	H_2O-3

1. The haem propionates are called inner (HP-7) and outer (HP-6) in some papers.
2. Except for Thr49N and Gly41N the listed residues interact with the propionates via their side-chains. Interactions with the other two residues are via their main-chain peptide NH.
3. H_2O-3 is one of three buried water molecules. It is also hydrogen bonded to Arg38. H_2O-1 interacts with Asn52, Tyr67 and Thr78. H_2O-2 is located in a different part of the structure, close to the peptide chain from residue 27–29 where it is partly exposed.

a semi-empirical method and is compared with the chemical shift difference of the nuclear resonance in ferricytochrome *c* and its diamagnetic analogue, ferrocytochrome *c*. This chemical shift difference is referred to below as the redox-state shift.

The redox-state shift is formally defined using the equation

$$\Delta_R = \delta_p - \delta_d \tag{10}$$

where Δ_R is the redox-state shift, δ_p is the chemical shift of a resonance in the paramagnetic molecule while δ_d is the chemical shift of the same resonance in the diamagnetic reference. This defines a downfield shift from the diamagnetic to the paramagnetic species as a positive quantity.

Ideally the paramagnetic molecule and its diamagnetic reference would have identical structures and local diamagnetic properties. The observed shift can then be expressed as a sum of two terms, describing the dipolar (through space) and Fermi-contact (through bond) interactions of the nucleus and the unpaired electron spin.[19] The contact term is scalar and is rapidly attenuated by intervening chemical bonds. In ferricytochrome *c* it is only expected to be of significance for resonances of the haem group and its ligands, Cys14, Cys17, His18 and Met80, and it has been estimated that only about 0.2% of the unpaired electron spin density is delocalised into orbitals of the ligands.[20] Consequently, for protons other than those of the haem

group and its ligands, this delocalization does not significantly affect the treatment of the unpaired electron as a single point dipole centered on the iron atom.

We will use the NMR spectrum of ferrocytochrome *c* as a diamagnetic blank for the spectrum of ferricytochrome *c*. The structures of both these molecules have been determined to high resolution (1.5 Å and 1.8 Å, respectively) in the solid state and are found to be very similar.[12] The significant structural differences in the crystal are limited to changes in the orientations of amino acid side-chains at the protein-solvent interface, and some changes of internuclear distances within the protein around the haem propionic acid groups, which occur without requiring extensive repacking of side-chains. In solution the measurement of torsional angles and internuclear distances by NMR has also demonstrated that a large amount of the protein structure is unaffected by the oxidation state change. However the rearrangement around the bottom of the haem crevice is more extensive in solution than in the crystal and an additional redox-dependent conformational change has been observed at the C-terminus (see below). Furthermore a comparison of the haem ring-current shifted resonances of cobalticytochrome *c* and ferrocytochrome *c* has shown that the effects of metal charge and donor/acceptor properties on the haem ring current and electric field are small.[21] For most residues the difference in chemical shift of a proton between the oxidized and reduced molecules, Δ_R, will therefore be dominated by the pseudocontact shift term. A large number of NMR resonance assignments are available for both ferricytochrome *c* and ferrocytochrome *c*[22,23]; consequently Δ_R is known for over 100 resonances of tuna cytochrome *c*. In addition the redox-state shifts of many resonances have been observed directly in a two-dimensional NMR EXCTSY experiment.[24]

The pseudocontact shift of a nucleus due to the anisotropic magnetic moment of the unpaired electron spin can only be easily observed in the NMR spectrum if the electronic spin lattice relaxation time is short ($T_{1e} < 10^{-10}$ s). Low-spin Fe(III) complexes satisfy these conditions of anisotropy and relaxation time, and for the purposes of NMR transitions only the average of the electronic magnetic moment over a time that is long compared with T_{1e} need be considered. The time-averaged magnetic moment of the electron is given by the magnetic susceptibility and a calculation of the pseudocontact shift, Δ_{PC} is then given by[19]

$$\Delta_{PC} = \left\{ \frac{1}{3}\left[\chi_z - \frac{1}{2}(\chi_x + \chi_y) \right] \frac{(3\cos^2\theta - 1)}{r^3} + \frac{1}{2}(\chi_x - \chi_y) \frac{\sin^2\theta \cos 2\phi}{r^3} \right\} \quad (11)$$

where χ_i are the magnetic susceptibilities along the principal axes and r, θ and ϕ relate the nucleus under study to the principal axes as illustrated in Fig. 5.

Unfortunately, susceptibility tensor components are unavailable for cytochrome *c*. However in this case there is only one thermally populated multiplet and very small mixing of excited states into the ground state and the susceptibilities may be replaced by electronic

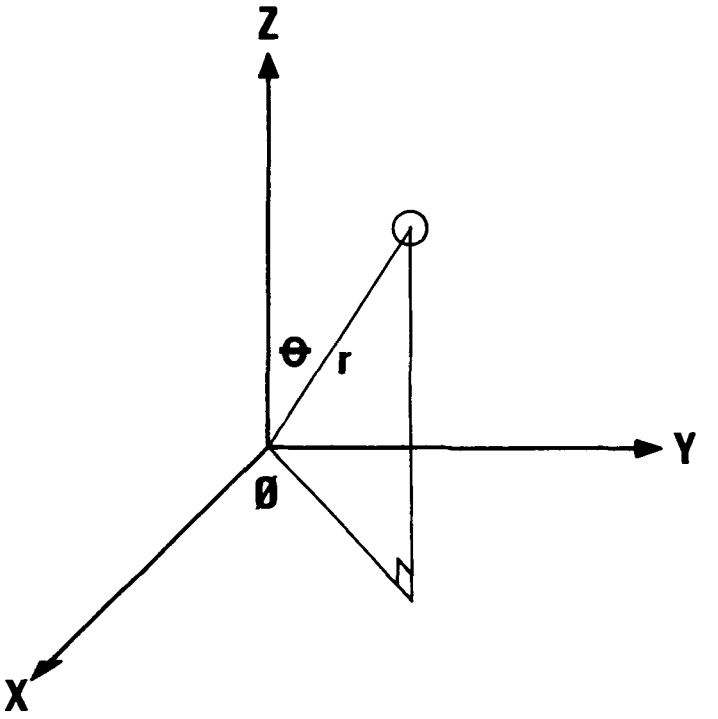

FIGURE 5 The coordinate system of the pseudocontact shift equation (20). The electron-spin magnetic moment is taken to be localized at the origin and the open circle represents the position of a nucleus in the principal axis system.

g-values, measured from an electron spin resonance (ESR) spectrum according to Eq. (12).

$$\chi_i = \frac{N\beta^2 S(S+1)}{3kT} g_i^2 \tag{12}$$

The magnitude and orientation of principal components of the g-tensor of a single crystal of horse ferricytochrome c have been measured at 4.2 K.[25] In order to calculate pseudocontact shifts at room temperature an effective g-tensor is defined whose principal components are given by

$$g_i^{\text{eff}} = \frac{\Sigma_j g_i^j \exp(-E_j/kT)}{\Sigma_j \exp(-E_j/kT)} \tag{13}$$

where j is allowed to vary over all occupied electronic states and g_i^j represents a g-tensor component of the jth electronic state.

The pseudocontact shift contribution Δ_{PC} (Eq. (11)) can now be expressed in terms of effective g-values (Eqs. (12) and (13)) as follows

$$\Delta_{PC} = \frac{-N\beta^2 S(S+1)}{9kT} \left\{ \left[g_z^2 - \frac{1}{2}(g_x^2 + g_y^2) \right] \frac{(3\cos^2\theta - 1)}{r^3} + \frac{3}{2}(g_x^2 - g_y^2) \frac{\sin^2\theta \cos 2\phi}{r^3} \right\} \tag{14}$$

Elsewhere[26] we show in detail how we have obtained the best set of g-values and their orientations under our experimental conditions. These differ slightly from the values obtained from a single-crystal study at 4 K due to first-order and second-order Zeeman effects and structural changes in the protein on the removal of crystal packing constraints.

The calculated pseudocontact shift, Δ_{PC}, is plotted against the solution redox-state shift Δ_R in Fig. 6, for all resonances of tuna cytochrome c which are firmly assigned in both oxidation states. The calculations were performed using the 1.8 Å "outer" coordinate set of tuna ferricytochrome c (Table II) as a model of the solution structure and good agreement between the observed and calculated shifts is obtained over the full shift range (−3 ppm. to +3 ppm.).

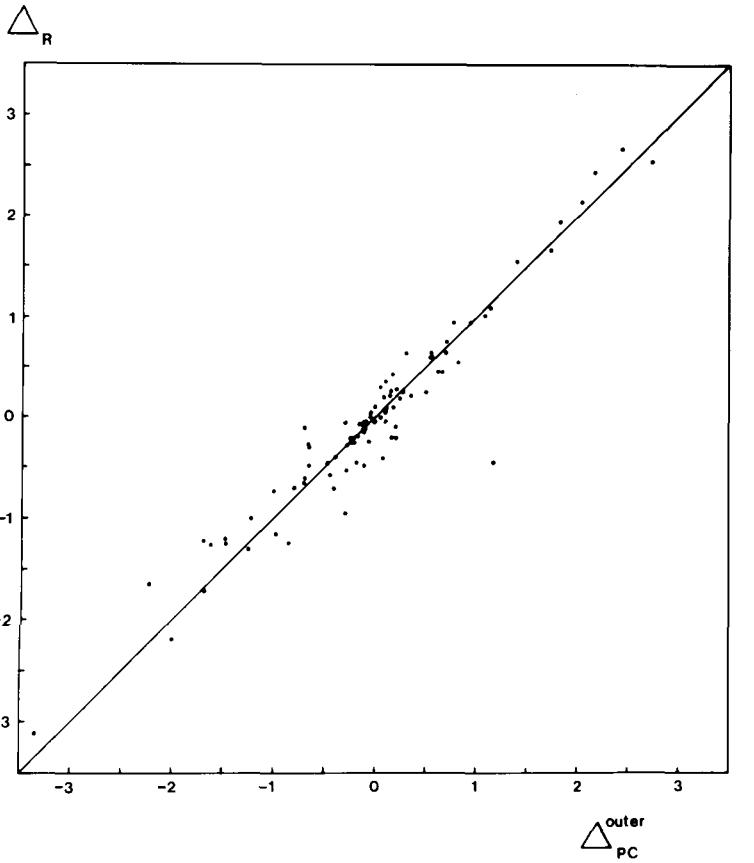

FIGURE 6 Plot of the observed solution redox-state shifts (Δ_R) for resonances of tuna cytochrome *c* against the corresponding calculated pseudocontact shifts obtained using Eq. (14) and the "outer" set of ferricytochrome *c* x-ray coordinates. The solid line is for reference only and does not represent a theoretical fit. (Taken from Ref. 26.)

Comparable agreement is obtained if either of the remaining high-resolution crystal structures (Table IV) is used. Within 10 to 15 Å of the ferric ion, the pseudocontact shift is an extremely sensitive structural tool and is capable of detecting small changes in protein conformation. The data of Fig. 6 demonstrate that the solution orientations of the haem packing residues (Fig. 4) are accurately represented by the x-ray coordinates. This is emphasized by examining the pseudocontact shifts of these residues when the calculations are

TABLE IV

Comparison of observed and calculated pseudocontact shift for tuna cytochrome *c*

Haem Packing Methyl Group	Δ_{PC}^{outer}	Δ_{PC}^{inner}	$\Delta_{PC}^{reduced}$	$\Delta_{R}^{solution}$
Leu32δ_1	+2.75	+2.05	+3.16	+2.55
Leu32δ_2	+2.05	+1.88	+2.18	+2.16
Leu35δ_1	−0.18	−0.21	−0.16	−0.25
Leu35δ_2	−0.44	−0.56	−0.39	−0.21
Leu64δ_1	−0.59	−0.50	−0.53	−0.78
Leu64δ_2	−0.86	−0.72	−1.02	−1.25
Leu68δ_1	−1.68	−1.93	−2.25	−1.72
Leu68δ_2	−3.34	−3.19	−4.70	−3.11
Ile85γ_2	−0.66	−0.63	−0.67	−0.50
Ile85δ	−0.98	−1.42	−1.22	−1.16
Leu94δ_1	−1.23	−1.31	−1.17	−1.00
Leu94δ_2	−2.24	−2.25	−2.21	−1.66
Val95γ_1	−0.40	−0.41	−0.39	−0.39
Val95γ_2	−0.70	−0.67	−0.74	−0.66
Leu98δ_1	−0.63	−0.79	−0.19	−0.30
Leu98δ_2	−1.70	−1.87	−1.43	−1.23

performed using a variety of x-ray structures amongst which the r.m.s. displacements of the haem packing residues are less than 0.3 Å on the average (Table IV).

In some cases the pseudocontact shifts of the haem packing methyl groups change by more than 1 ppm as a result of the small crystallographic differences. When the solution redox-state shifts of these methyl groups are compared with the pseudocontact shift data it is found that, for most residues, the range of calculated pseudocontact shifts is greater than the minimum difference between the observed and calculated shifts. Thus, the change in the position relative to the haem of the haem contact residues between the crystal and solution states is probably less than 0.3 Å. However, this procedure assigns all the observed discrepancy to changes in the pseudocontact shift caused by variations in geometry between the crystal and solution. If other sources of error in the calculations such as the evaluation of the *g*-tensor orientation and magnitude in solution could be taken into account the mean positional changes of these residues are expected to be considerably smaller than 0.3 Å.

Those haem packing methyl groups for which the solution redox-state shift is consistently and significantly different from the calculated pseudocontact shifts are Leu64δ_1, Ile85γ_2, Leu94δ_1 and Leu94δ_2 (Table IV). Although it is possible that these residues move by more

than 0.3 Å between the crystal and solution structures it is also possible that structural changes of neighboring residues between oxidized and reduced cytochrome *c* in solution give rise to diamagnetic contributions to the redox-state shifts of these groups which are not embodied in the pseudocontact shift calculations. In particular, NMR studies have shown the region around Leu94 and Ile85 to be relatively mobile.

Overall the correlation of the solution redox-state shift with the crystal-based pseudocontact shift has shown that the gross structure of the protein (e.g., the points at which the polypeptide chain cuts the rhombic shift cone) is maintained in solution. In addition the positions of most of the methyl-containing haem packing residues change by less than 0.3 Å. However, little information concerning the positions of residues far from the haem is obtained from this procedure and this includes many residues on or near the protein surface which have previously been implicated in the redox-state conformation change. To study these residues we turn to the application of nuclear Overhauser enhancements (NOE) and coupling constant measurements.

(ii) Nuclear Overhauser Enhancement Studies. While a global view of structure in solution can be obtained from paramagnetic shift (or relaxation) probes, detail at the level of ± 1 Å is not discoverable, unless in regions close to the shift or relaxation center. However, in all regions of the protein we may use NOE effects between NMR resonances to make deductions concerning the scalar distances between groups. Under the conditions of protein NMR experiments the effect reaches only some 4–5 Å from the irradiated proton and it is therefore extremely useful in defining local structural detail. Once again we proceed by comparing the predictions of the crystal structure with the NMR observations in solution.

Figure 7 shows some residues between which NOE effects are expected (or not expected) from crystallographic data and compares this with our observations. There is good correlation between the two quadrants of Fig. 7, reinforcing the conclusion that the structures of cytochrome *c* in solution and in a crystal are similar and that in general any local differences must involve motions of groups of less than 1 Å. Most of the NOE data of Fig. 7 which may not be interpreted on the basis of the crystal structures, and using a 4 Å cut off, involve small effects between protons separated by 4–6 Å.

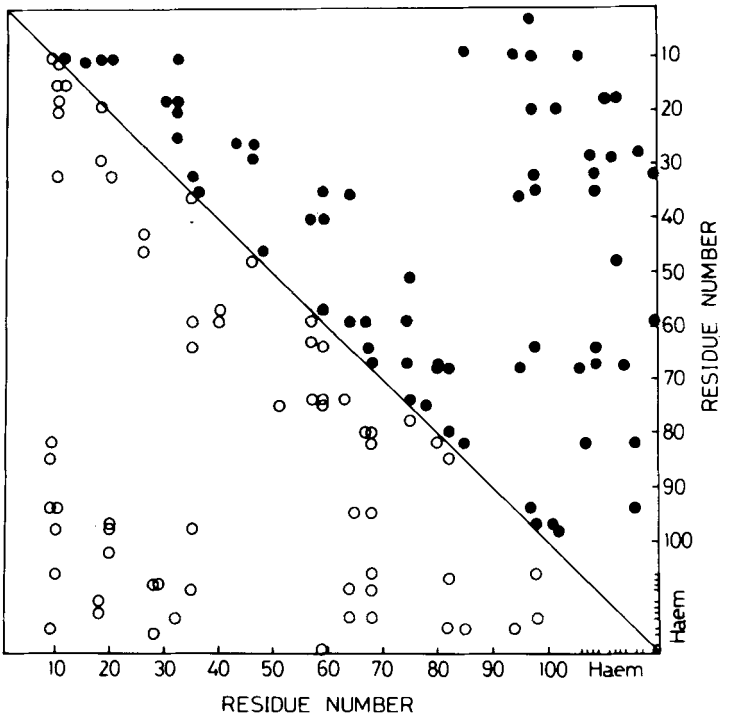

FIGURE 7 A comparison of the observed and expected NOE effects of tuna cytochrome *c*. The filled circles of the upper quadrant indicate amino acid residues separated by less than 4 Å in the tuna cytochrome *c* crystal structures. The open circles represent NOE effects (excluding intrahaem NOE's) observed in the NMR spectra of tuna ferrocytochrome *c* and ferricytochrome *c*.

These effects may therefore be accounted for by minor changes in the structure, by allowing structural mobility or by the inclusion of spin diffusion.[27] Only the observed NOE patterns of Ile57, Thr40 and Thr63 require significant changes of their side-chains and this is considered further here.

Figure 8 shows NOE difference spectra produced by the irradiation of the resonance of Ile57δ in tuna ferricytochrome *c* and tuna ferrocytochrome *c*. In ferrocytochrome *c* NOE's are observed to methyl resonances of two other residues, Thr40 and Thr63, where only one such effect, to Thr40, is predicted from measurements of the ferrocytochrome *c* crystal structure.[12] In ferricytochrome *c* an NOE is

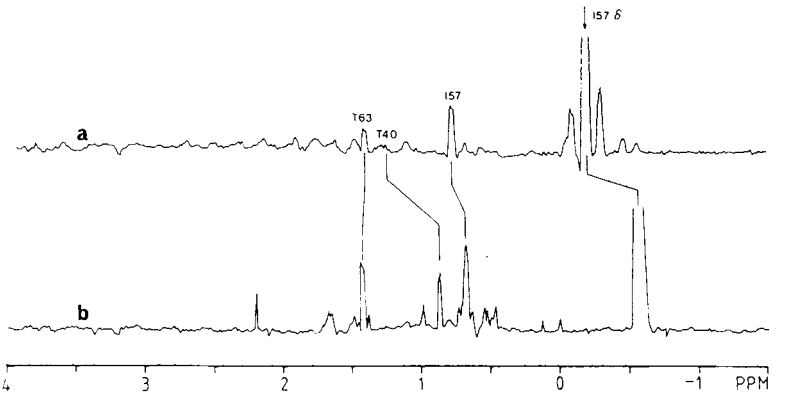

FIGURE 8 Structural differences between ferrocytochrome *c* and ferricytochrome *c* in solution demonstrated using NOE difference spectroscopy. Spectrum (a) shows the NOE effects observed in tuna ferricytochrome *c* on irradiation of the resonance of Ile57δ and indicates the proximity of the γ-methyl groups of Thr63 and Ile57 to the Ile57δ protons. Spectrum (b) shows the NOE pattern obtained on irradiation of the resonance of Ile57δ in tuna ferrocytochrome *c*. In this oxidation state an additional methyl group, that of Thr40, is packed around Ile57δ.

observed to only one such methyl resonance, that of Thr63, while measurement of the ferricytochrome *c* crystal structure indicates that NOE effects should be observed at the resonance of Thr40 only.

The NOE data indicate that in solution the distance between the δ methyl group of Ile57 and the γ methyl group of Thr40 is redox-state dependent, being greater than 4 Å in tuna ferricytochrome *c* and less than 4 Å in tuna ferrocytochrome *c*. This redox-state conformation change does not occur in crystals of cytochrome *c* where the Thr40γ and Ile57δ methyl groups are constrained to be within 3.5 ± 0.3 Å of each other in both oxidation states. In addition the distance between the methyl groups of Thr63γ and Ile57δ is less than 4 Å in solution yet is 4.9 Å in crystals of cytochrome *c*. Within the limits of accuracy of the NOE and x-ray data, this distance is not redox-state dependent in either crystal or solution.

At present it can be stated with certainty that the redox-state changes in this region are real but there may be contributions both from static changes in the structure and from the presence of a number of local conformations in solution which are in rapid equilibrium with each other and whose relative populations are redox-state and solution/crystal dependent. Further work must be done to establish

the relative contributions of changes in average structure and local dynamics to the redox-state conformation change. The apparent structural changes are described more fully in a subsequent section.

(iii) Coupling Constant Analysis as a Structural Tool. A number of α CH resonances have been resolved in the NMR spectrum of tuna cytochrome *c* and assigned to specific residues.[22,23] Under conditions where all amide protons are exchanged for deuterons (NH → ND), the multiplet structure of these resonances may be analyzed to give values of three-bond coupling constants ($^3J_{\alpha\beta}$) representing scalar interactions between the α and β protons. The value of the coupling constant may be related to the dihedral angle θ, using the equation[28,29]

$$^3J_{\alpha\beta} = A\cos^2\theta + B\cos\theta + C \qquad (15)$$

The values of *A*, *B* and *C* have been measured using a series of rigid model compounds[30] and were taken to be 9.4 Hz, −1.4 Hz and 1.6 Hz, respectively. For the case of threonine only the calculated coupling constants were divided by 1.08 to allow for the electronegativity effects of the hydroxyl group at the C_β position.[30] From work on model compounds whose structure has been determined by x-ray analysis or minimum-energy calculations, it has been estimated[29] that these calculations are accurate to better than ±1 Hz.

The calculated and observed coupling constants are shown in Table V. In general the agreement is within 2 Hz. This implies that the dihedral angles describing the solution conformations of most residues are well represented by the values obtained from the crystallographic analysis. Furthermore the values observed for many residues, which are either > 10 Hz or < 3 Hz, suggest that the dominant rotamer in solution is staggered, with the α and β protons either *trans* or *gauche* to each other and that little rotational averaging of these conformers takes place. For residues where two β protons are present, one coupling constant is large and the other is small. These data demonstrate for cytochrome *c* a preference for staggered conformations of side-chains in solution which has previously been observed in analogous NMR studies of the β-sheet structural unit of lysozyme,[31] in the solid state by analysis of the x-ray crystal structures of many proteins[32,33] and from theoretical studies.[34]

The discrepancies observed for two residues, Val11 of ferricyto-

TABLE V

Observed and calculated $\alpha\beta$ coupling constants (Hz) of tuna cytochrome *c*

Residue	$^3J_{\alpha\beta}$ Ferrocytochrome *c* obs	calc	$^3J_{\alpha\beta}$ Ferricytochrome *c* obs	calc
Val11	11.73	12.27	9.39	12.16
His18	?	12.16, 2.26	10.30	11.66, 1.74
Thr19	?	2.86	< 3.0	2.96
Val20	3.0	1.98	?	1.64
Val28	10.57	12.40	11.03	12.14
Leu32	10.80	12.23, 2.33	?	12.37, 2.63
Leu68	11.70	12.10, 2.14	10.59	11.50, 1.67
Thr78	< 4.0	3.61	8.22	2.64
Ile81	9.97	12.32	10.97	12.31
Val95	?	11.75	10.30	11.80

obs = observed; calc = calculated.
? not determined.

chrome *c* and Ile81 of ferrocytochrome *c* are greater than 2 Hz but less than 3 Hz, with the observed coupling constant being smaller than the calculated value (Table V). Both these residues lie on the surface of the cytochrome *c* molecule. In the absence of side-chain hydrogen bonding, the differences in energy between rotamers and the barriers to their interconversion are likely to be small for such residues. The observed reduction of the coupling constant may result from significant populations of *gauche* rotamers in solution which are either absent in the crystal or seen only as small redistributions of electron density between the heavy atom positions of the dominant *trans* conformer. For both Val11 and Ile81 a change in the average value of θ of less than 25° is required to bring the experimental and calculated coupling constants into exact agreement.

The discrepancy of 5.6 Hz between the observed and calculated $^3J_{\alpha\beta}$ coupling constants of Thr78 in ferricytochrome *c* represents a change of 44° in the average value of θ between the solution and crystal conformations. Thr78 is a completely conserved, partially buried residue which is part of a rigid structural unit (the 75–78, 3_{10} bend; see Fig. 3) and whose side chain is hydrogen bonded to the carboxyl group of haem propionate-6 in all the crystal structures of cytochrome *c* currently available (Table II). It is likely that this hydrogen bond, which stabilizes the buried propionic acid group, is maintained in solution thus limiting the extent to which the Thr78

side-chain may be rotated on dissolving the crystal. For this reason we believe that some rotation of the polypeptide backbone must occur around residue 78 of ferricytochrome *c* on the removal of crystal packing forces. Although the effects of this rotation may be rapidly attenuated further up the polypeptide chain by adjustments of backbone torsion angles and atom positions in the deformable loop formed by Lys79 to Lys87, the presence of a rigid 3_{10} bend between residues 78 and 75 may lead to more extensive changes in atom positions below residue 78. For example, if the rotation occurs without movement of Thr78γ and without deformation of the 3_{10} bend, the α carbon atom of Ile75 will move by 3.8 Å. Although this calculation represents an upper limit, the effect of any such motion will be transmitted to the α-helix formed by residues 74 to 70, whose side-chains (notably that of Tyr74) make contact with the side chains of residues 56 to 60. Further transmission of the motion may occur *via* the helix formed by residues 61 to 69 before the motion is dissipated in the 50's loop (see Fig. 3).

Additional work is required to characterize these changes but it is clear that any reorientation of Thr78 will be accompanied by further structural changes at the base of the haem. Evidence that such changes do occur on dissolving the crystal has been given in the previous section where it was shown that the intramolecular contacts between Thr63, Ile57 and Thr40 change when crystalline ferricytochrome *c* is dissolved, while smaller changes are observed when ferrocytochrome *c* is dissolved. These contacts, as well as the Thr78C_α-C_β dihedral angle, alter on oxidation or reduction of cytochrome *c* in solution and may contribute to the required structural relaxation during electron transfer.

C. The Surface of Cytochrome *c*

The analysis of structure which we have made so far is largely confined to the *internal* hydrophobic residues. On the surface are residues of a very different character, often hydrophilic and charged, e.g., lysines and glutamates. Because these residues are charged, exposed to water and relatively long chain, they are not readily confined structurally. For example, the conformations of some of the lysines of cytochrome *c* vary greatly from one crystal structure to another and from one molecule to another in the same unit cell. We conclude

that a simple representation in structural terms does not have the same value for the description of a surface of a protein as it has for the inside.

We are primarily interested in the surface because it is a binding area for other molecules. Thus a useful description of the surface is in terms of the available binding sites (i.e., effective potential-energy wells) into which various types of molecule will go.[7,35] A start in this direction is made if we consider the likely partners for the surface knowing that the interaction must take place in water and must be selective for a limited set of molecules. Protein/protein interaction will clearly include both electrostatic and hydrophobic binding terms, although it is the former that are generally more important. Therefore we search for the potential-energy wells developed on the surface by using probe molecules of variable size, shape and polarity. Experimentally this is done by choosing reagents such as an anion, e.g., $[Cr(CN)_6]^{3-}$, to look for the positively charged parts of the surface, a cation, e.g., $[Cr(NH_3)_6]^{3+}$ to look for the negatively charged parts of a surface and molecules such as $[Cr(AcAc)_3]^0$ to look for more hydrophobic regions. Notice that in each case the probe molecule is roughly spherical so that the method is equivalent to a theoretical ball "rolled" over the surface to inspect potential-energy functions. They have no particular stereochemical features except their sizes. Experimentally, the shape of the ball can be altered by using asymmetric reagents, e.g., $[CrEDTA.H_2O]^-$. Note that the complexes illustrated here all contain Cr(III). This metal ion is chosen because it is an NMR relaxation reagent and maps out the surface to which it binds by broadening the lines in an NMR spectrum.[7]

We have observed[7] that $[Cr(CN)_6]^{3-}$ has at least six sites at which it binds to cytochrome *c*. The sites are the same as those for $[Fe(CN)_6]^{3-}$, a reagent which has often been used in electron transfer studies. The significance of this observation is considered in Section 7.A, which deals with rates of electron transfer. Here we note that we have found areas on the surface of cytochrome *c* which have a positive potential. Areas of negative potential have been using located cation probes. In this way the surface is represented by a mosaic of dynamic patches, Fig. 9. The patches do not move around but contain dynamic side-chains. It is this mosaic which can provide a number of valuable properties both for the dynamics and the selectivity of binding of protein/protein interaction.[35-37]

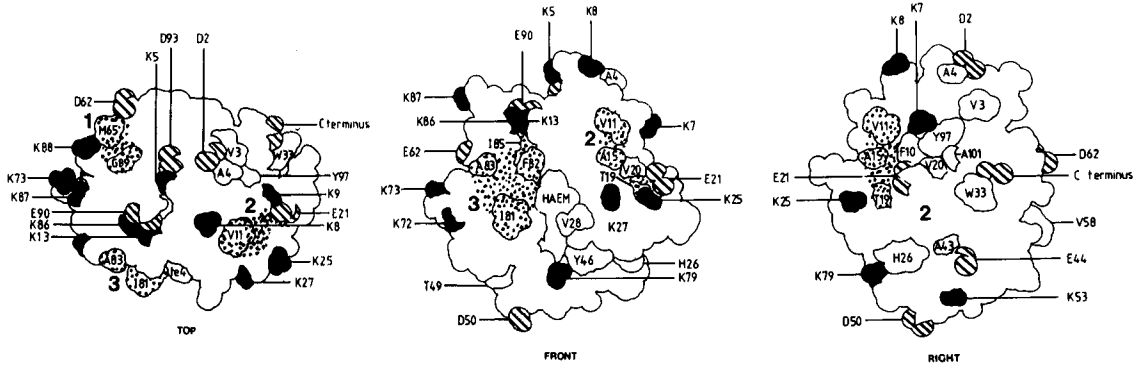

FIGURE 9 Representation of the three major anion binding sites on tuna cytochrome *c*. The space-filling diagrams illustrate the positions of negatively charged groups (striped) and positively charged groups (solid). Important residues with assigned NMR resonances are shown in outline. The stippled residues are those affected by low concentrations of probes of the type $[Cr(CN)_6]^{3-}$ and $[Fe(edta)(H_2O)]^-$.

D. Redox-State Conformational Changes

The structures of ferricytochrome *c* and ferrocytochrome *c* determined by NMR and x-ray crystallography represent the fully relaxed, time-averaged, ground-state conformations under the particular conditions of *p*H, ionic composition and intermolecular contacts, and do not correspond to the activated structures of reactive complexes. Nevertheless, a thorough definition of the structural differences between the two ground states in solution will indicate some of the regions of the protein which take part in the activation process.

We have alluded to some of the redox-state conformation changes in previous sections. The main region of change, as indicated by both x-ray and NMR studies, is at the base of the haem (Fig. 10) and involves certain haem packing residues and the 50's loop and helix. However, the two techniques disagree as to the extent and nature of the changes with the x-ray structures[12] indicating that they are confined to the left-hand side of the protein around Met80 (as viewed in Fig. 10) and the base of the protein, while the NMR studies[21,26] indicate that the changes extend to the N and C termini of the polypeptide chain. The main reason for this discrepancy is likely to be that the crystal packing distortion referred to previously dampens the conformational differences. This is a result of the main crystal intermolecular contact region involving the 50's residues in both ferricytochrome *c* and ferrocytochrome *c*.[11,37] Thus although we can list the regions of the structure that are perturbed, we cannot yet give a precise atomic description of the magnitude of the changes. However, in most cases atomic displacements are $\leqslant 1$ Å. A summary of the affected regions of the structure is given in Fig. 10.

For convenience we shall describe the redox-linked conformation change as if there were a single mechanism involving a sequence of well-defined structural changes. In reality these changes will not be sequential, but will be, to some degree, cooperative. In addition, since the electron transfer is probably not adiabatic, there is no unique reaction pathway from the occupied vibrational states of the reactants to those of the products.

Upon adding an electron to the Fe(III) ion of ferricytochrome *c*, an electrostatic relay comprising of Fe(III)–HP-7–Arg38 within the protein is modified so that the buried charge pair (HP-7–Arg38) is destabilized.[38] A small rearrangement must then occur at the base of the haem group in order to restabilize the ion pair through charge–

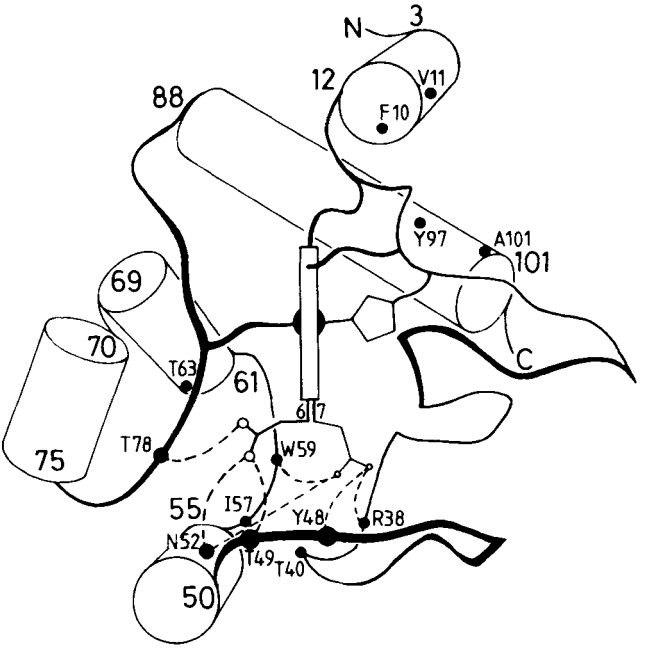

FIGURE 10 Structural diagram of mitochondrial cytochrome *c* summarizing some of the features important in the redox-state conformation change. One of the possible haem propionate interaction schemes is illustrated by the broken lines; the cylinders represent α-helices. Residues known from NMR studies to be affected by the redox-state conformation change are: Phe10, Val11, Thr40, Ile57, Trp59, Thr63, Thr78, Tyr97 and Ala101.

dipole interactions. The question arises as to whether this movement is part of the trigger process for the electron transfer or part of a subsequent conformation change. It is also not clear if changes in the Fe–S bond length and angle are involved in the trigger. In a previous paper[1] we reviewed the spectroscopic evidence supporting such a role for the Fe–S bond and contrasted this with the x-ray and EXAFS data which argue against any change in the Fe–S link. There we suggested that a redox-dependent rotation about the Fe–S bond might satisfy both sets of data. Further experiments are required to resolve this problem. Certainly the Fe–S bond is less stable in the oxidized state and breaks in the range 50–80°C.[1,39]

Once the conformation change has been initiated, it is transmitted throughout the protein by small adjustments in the orientations of

amino acid side-chains and the relative positions of α-helices. Thus, movement of the 50's loop and residues on the left-hand side of the protein perturb the 60's helix which, via side-chain interactions with the C-helix, perturb the C-helix and then the N-helix. Similar long-range perturbations have been demonstrated using selective chemical modification of particular residues; for example,[40] carboxymethylation of Met65 in the 60's helix leads to a structural change around Phe10 (N-helix) and Tyr97 (C-helix).

E. Summary of General Structural Features

1. The haem is almost completely buried by the protein cage (Fig. 3).
2. The overall protein fold in the two oxidation states is similar.
3. There are small redox-state conformational differences of internal side-chains in several parts of the protein with the major changes located at the base of the protein around the haem propionates (Fig. 10).
4. The surface of the protein cannot be defined in strict structural terms.
5. There are a variety of dynamic modes to the protein structure that may be important for electron transfer. This is elaborated in the following section.

F. The Dynamics of Cytochrome *c*

In Section 2 we described the possible need for vibrational and conformational activation of the electron-transfer complex before electron transfer took place. Although the protein complex has very many vibrationally and conformationally excited states, electron transfer is restricted to those states in which the energy of the electron is the same at the donor and acceptor sites. Thus in Fig. 11, which represents some conformational states of the ferricytochrome *c*/ferrocytochrome *c* complex, the electron self-exchange reaction might only occur when the complex reaches point *X*, and nowhere else.

In order to understand the electron transfer process we are required to find the vibrational modes and/or conformational equilibria which can affect the haem redox potential, although we can ignore any conformational changes which occur on time scales longer than the

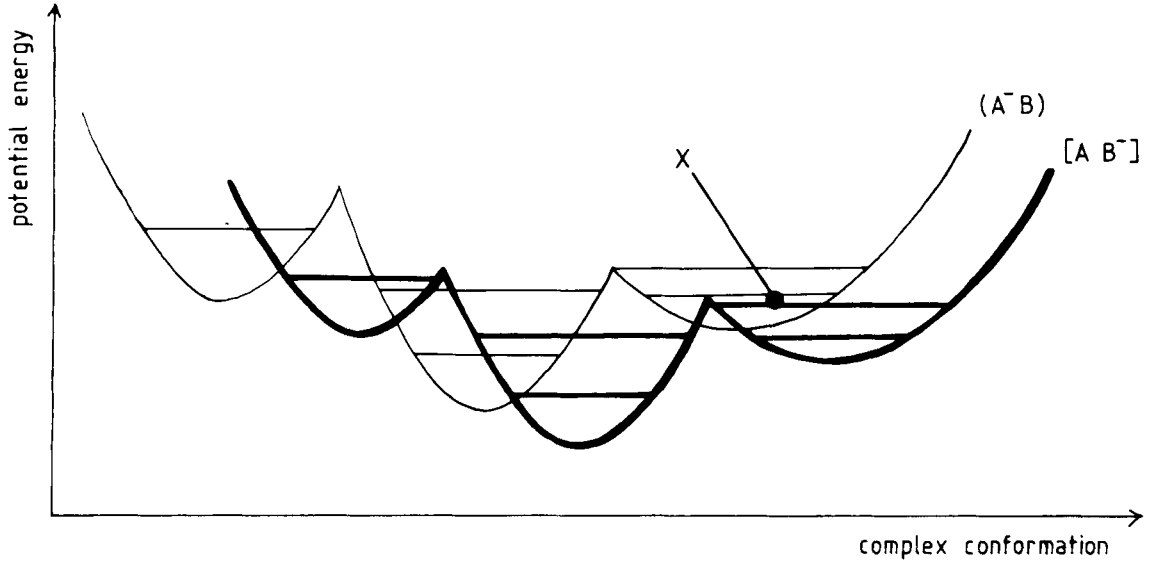

FIGURE 11 Potential-energy surfaces for reactant and product complexes of electron transfer. The surface of the product complex [AB^-] is shown using a bold line while that of the reactant complex (A^-B) is represented by a light line. Electron transfer, {A^-B} → {AB^-}, occurs at a single point X on the diagram. The complex conformation at this point has the property that the energy of the electron is the same at both the donor and acceptor sites. In a real system there will be many ways in which such a point as X can be reached.

overall electron-transfer process. For the reactions of cytochrome *c* with its physiological redox partners the rate of electron transfer within the active complex is in the range 10^2–10^4 s^{-1} (see Section 6) and we can therefore neglect slow processes (rate $< 10^2$ s^{-1}) such as protein unfolding, ligand exchange and the rotations of many aliphatic and aromatic side-chains within the protein.

The infrared spectrum of cytochrome *c* [G. R. Moore, P. Tonge and C. Wharton (unpublished data)] confirms the presence of many vibrational modes with frequencies in the range 10^{12}–10^{14} s^{-1}. These are the motions studied by x-ray crystallography[41,42] (B-factors) and arise from small oscillations of atoms or small groups of atoms about potential-energy minima. Only those vibrations which involve the porphyrin ring or the haem ligands or lead to the movement of local dipoles and charges will affect the energy of the electron at the iron atom and need be considered further. If electron transfer does occur from a state of these oscillators which is populated under physiological conditions then the electron-transfer rate will reflect a tunneling event and will not be an activated process.[43] However if electron transfer requires population of high-energy vibrational states or molecular conformations the rate will be activated and we might expect to be able to correlate the activation energy parameters of electron transfer with those of the conformational change.

The rates of conformational changes may be studied using NMR. In cytochrome *c* the large chemical shift differences between pairs of methyl groups from the same leucine or valine residue have confirmed that most of the interior of cytochrome *c* has a lack of mobility which resembles a crystalline solid rather than the conventional "oil-drop" model of protein cores. In these regions asymmetric side-chains flip at rates less than 10^2 s^{-1}.

Further dynamic information is obtained from the eight tyrosine/phenylalanine residues of tuna cytochrome *c*. These residues are distributed throughout the protein and demonstrate a range of flip rates in the NMR spectrum.[44,45] Four aromatic rings are packed together in two pairs (Phe10/Tyr97 and Tyr46/Tyr48) on the right-hand side of the haem plane and near the molecular surface, where they undergo relatively slow ring flips ($< 10^2$ s^{-1}). A fifth residue, Tyr67, is buried deep inside the protein and begins flipping at an appreciable rate only at temperatures close to the denaturation point. The activation energy for these ring flips is of the order of 100 kJ/mole.

These motions are too slow to contribute to the vibrational relaxation of the protein during electron transfer under normal solution conditions, and remain slow when the protein is complexed with small inorganic redox reagents.

The remaining three aromatic amino acids of tuna cytochrome *c*, Phe36, Tyr74 and Phe82, undergo rapid flipping with, for Phe82, a rate in excess of 10^4 s^{-1}. Phe36 is somewhat exposed to solvent at the rear of the molecule and 12 Å from the haem center. Although its flip rate is in the correct range for vibrational activation/relaxation of the electron-transfer complex there is no obvious mechanism by which the two processes may be coupled. In contrast, Tyr74 is partially exposed to solvent at the left rear corner of the molecule in a region of the protein whose conformation is known to be sensitive to the redox state of the iron atom. In Section 5D it was proposed that this conformation change is coupled to the redox state via an electrostatic interaction between haem propionate-7 and the iron atom. This coupling could also be used to relax the redox center at the rate of flipping of Tyr74. Finally, Phe82 is partially exposed to solvent at the front of the molecule, where it lines the left-hand side of the haem crevice. Due to the proximity of Phe82 to the haem center and the iron ligand Met80, it is probable that the flipping of the side-chain of this residue is also coupled to the vibrational activation/relaxation of the reaction center.

Motions on this time scale are also reflected in the behavior of the resonance of haem methyl-3 in the NMR spectra of some ferricytochromes *c*.[46] At present there is no explanation of the nature of this motion, e.g., whether it involves the deformation of the porphyrin ring or is a reflection of structural changes in the protein residues (including Phe82) around this edge of the haem group. However, in horse ferricytochrome *c* it is coupled to the protonation state of His33.[39]

Additional dynamic information is obtained by studying the temperature dependence of the chemical shift of resonances in the NMR spectrum of ferrocytochrome *c*. In a diamagnetic protein, proton resonances are shifted from their unperturbed positions due to the presence of nearby magnetically anisotropic groups (e.g., aromatic rings) within the molecule. Any changes in the shift of a resonance will reflect the effects of changes in the average orientation of the corresponding proton with respect to a magnetically anisotropic

group. The positions of most resonances of ferrocytochrome *c* are independent of temperature over the range 20–80 °C, indicating that no major structural changes take place. However, two residues, Ile57 and Ala101, have temperature-dependent chemical shifts. These residues are in different regions of the protein structure of which one (near Ile57) has been implicated in vibrational activation and relaxation of the electron transfer. The observed change in average position of the methyl group with increasing temperature may be due either to the excitation of a highly anharmonic vibrational mode with a frequency $< 10^{11}$ s^{-1} or to the population of other rotamer states[47] and they reflect the looser packing of protein side-chains in these regions.

In conclusion, the dynamic properties of cytochrome *c* in both oxidation states encompass motions which occur over a wide time scale, from the vibrations of individual bonds (frequency $\sim 10^{14}$ s^{-1}) to the rotations of some aromatic rings (rate $\leqslant 10$ s^{-1}). In principle all motions of frequency or rate greater than 10^2 s^{-1} could contribute to the movement along the reaction coordinate of electron transfer although in practice only those motions which affect the energy of the electron at the iron atom need be considered. These motions include the vibrations of the iron–ligand bonds and those conformational changes which lead to the observed structural differences between ferricytochrome *c* and ferrocytochrome *c*. A more precise definition of the mechanism of the electron-transfer reaction requires further experimental work which must ultimately include measurement of the activation parameters for the reaction and their dependence on modifications (natural or artificial) to the protein sequence. Some of the experimental methods currently employed are discussed in the penultimate section.

6. BIOCHEMICAL ASPECTS OF THE ELECTRON-TRANSFER FUNCTION OF CYTOCHROME *c*

Although we have adopted a fundamental physical-chemical approach in describing the reactivity of cytochrome *c* we must remember that cytochrome *c* has been designed for a specific biochemical role: see the Introduction. In deciding what makes cytochrome *c* the chosen molecule to perform its particular biological function we shall con-

centrate on two properties: the time scale over which the protein functions and its redox potential.

Cytochrome *c* operates in an intermembrane compartment that is not well characterized.[48,49] Not only are the ionic strength and composition not clearly established, it also seems likely that cytochrome *c* remains attached to the membrane during some of its reactions while in others it dissociates into the aqueous phase. These topics are outside the scope of the present Comment but we note that they are of central importance to understanding the biological electron-transfer function of cytochrome *c*.

Chance[50] has carried out a detailed study of mitochondrial respiration and he claims that the rate of cytochrome *c* turnover is 10^2–10^3 s^{-1} *in situ*. This is in broad agreement with many *in vitro* studies of cytochrome *c* reacting with its purified reaction partners.[48,49] These reactions are usually limited by the dissociation of the product complex. Thus it appears that *in situ* the requirement is for the rates of off-reactions of cytochrome *c* to be $> 10^2$ s^{-1} and this also gives a requirement for electron transfer within the complex to be $> 10^2$ s^{-1}.

The fastest electron-transfer rate so far observed for cytochrome *c* is that for its oxidation by yeast cytochrome *c* peroxidase, which operates between the Fe(III) and Fe(IV) states.[51] The large redox driving energy for this reaction produces[52] an electron-transfer rate with cytochrome *c* of 10^4 s^{-1}. Since, in principle, the electron transmission step itself can be exceedingly fast, it is necessary to explain why the electron-transfer steps for cytochrome *c* are relatively slow. One possible reason is that the electron transfer is coupled to a conformational change (Section 5D; see Section 3 for the reasons that make it probable that the two processes are coupled). Yet, in part, this conformational change is a result of the unusual packing of the polypeptide chain around the haem which shields the haem propionates from the solvent. Thus it becomes apparent that an ideal biochemical electron transfer reagent for a specific reaction is not necessarily one that transfers electrons rapidly.

The question is then posed: what biochemical benefits accrue from reducing the rate of electron transfer for cytochrome *c*? However, this may not be the correct question to ask since the relatively slow electron-transfer rate itself may not be required, but be a consequence of some other desired property. Therefore, we must ask why the polypeptide wraps itself around the haem in the way it does (Fig. 3).

The almost complete burial of the haem is one means of raising its redox potential. A full description of the factors controlling protein redox potentials are beyond the scope of the present Comment but we wish to stress that there are two general mechanisms controlling such potentials. The first is the influence of the immediate ligands to the metal.[2] The second is the influence of the environment of the haem. This environmental control is usually described in terms of electrostatics with removal of the haem from the aqueous solvent being a major factor.[53,54] Thus we see that in order to have cytochrome *c* operating at the appropriate redox potential its haem has been buried within the protein cage. However, tuning of the redox potential could probably be achieved by burying the macrocycle only. Burial of the haem propionates does lead to a fine tuning of the redox potential[38] but the main effect of the burial is that it causes a redox-state conformation change (Section 5D). Thus it appears that the conformation change is a consequence of the "design."

In its biochemical pathways, cytochrome *c* interacts with a number of membraneous redox proteins to form relatively strong association complexes. There is specificity in these reactions in that ferricytochrome *c* has a slightly higher association constant for binding to cytochrome reductase than does ferrocytochrome *c*[55] while for cytochrome oxidase the affinity order is reversed.[56] We suggest that such redox-state-dependent association constants are a manifestation of the redox-state conformation change. Therefore it seems that cytochrome *c* has obtained some degree of biochemical specificity at the expense of its electron-transfer rate. Such specificity may have required a highly positive binding surface for its reaction partner, thus forcing the haem propionates to be buried with all the consequences we have seen for the electron-transfer rate. This includes the favorable generation of a conformational control switch.

7. EXPERIMENTAL APPROACHES TO THE ELECTRON-TRANSFER REACTIONS OF CYTOCHROME *c*

The kinetic parameters usually measured with cytochrome *c* are second-order rate constants. These are composed of two terms: the association constant for precursor complex formation and the first-order rate constant for electron transfer within the precursor complex. It is this latter rate constant that is described by Marcus theory (Fig. 1) and is our main concern in the present Comment.

In Section 2 we described the kinetic parameters which govern electron transfer within a preformed complex. They were:

(1) The free-energy difference between the reactant and product complexes, G_Δ (Fig. 1), which we shall refer to as the redox driving energy.

(2) The structural rearrangement energy, G_S, which corresponds to the free energy required to alter the bond angles, solvent cage, etc. of the reactant complex into those of the fully relaxed product complex.

(3) The transmission coefficient, κ, which will depend on the nature of the electron donor and acceptor centers, their distance apart, and the nature of the medium which separates them.

The redox driving energy will be determined by the precise nature of the reactant and product complexes and does not include the associated pre-equilibrium itself. When treating the reactions of large molecules we must also consider the possibility that there may not be a unique pair of reactant and product complexes through which reaction proceeds. The redox driving energy need not be equal to the redox potential difference of the separated species and may depend on *p*H, temperature, ionic strength and ionic composition in a completely different way. It is important to make this distinction when describing the *p*H and temperature dependence of the electron-transfer step (see Fig. 1).

The rearrangement energy arises from the small conformational adjustments which are required to make the electron transfer within the reactive complex isoenergetic. The electron is therefore transferred between vibrationally excited states of the reactant and product complexes. When describing the vibrational activation of proteins we must consider the possibility of cooperativity within the ordered structure and we should ask to what extent the observed structural differences between the redox forms of the isolated protein are reflected in the changes leading to activation. In the specific case of cytochrome *c* it is important to realize that some vibrational modes such as those involving the distortion of the Fe–S bond and the flipping of some aromatic rings have different frequencies in the two oxidation states. If these vibrational modes are coupled to the electron-transfer reaction then simple Marcus theory in which activation and relaxation processes are represented by parabolas of identical curvature (Fig. 1) is not applicable and Eq. (6) is no longer valid.

A critical test of this is the comparison of activation parameters for electron transfer with those of vibrational and conformational change.

The third problem, that of the distance and medium dependence of the transmission coefficient, κ, is perhaps the most intriguing of all. The redox centers of the mitochondrial electron-transfer chain are separated from each other by protein recognition surfaces, and the electron must travel distances of the order 10–20 Å during electron transfer. Much work remains to be done to establish the dependence of the transmission coefficient on the nature of the local environment, e.g., the presence or absence of conjugation, electronic dipoles, etc.

An investigation of the electron-transfer reactions of cytochrome *c* must begin by identifying the number of possible reactant complexes and their substrates. Further work could be aimed at identifying the contribution of each complex to the observed electron-transfer rate. This might be achieved by selective modification of the protein either chemically or via site-directed mutagenesis in order to block specific binding sites on the protein surface or by selective competition for binding sites using redox-inactive reagents. Since the protein can show cooperative effects over large distances, care must be taken to identify the effects of any modification on the structures and relaxation properties of all the possible electron-transfer complexes.

In fact a great many such experiments have been attempted and we shall describe these in outline. Two general approaches have been used. In the first, the surface of cytochrome *c* is probed using small, freely diffusing, inorganic complexes, and in the second, electron donors or acceptors which have been covalently linked to the protein surface are used in order to restrict the number of possible reactive complexes. Comparative studies within the first group have been particularly informative.[6,7] These have used both one cytochrome *c* with a series of small reagents, and one reagent with a series of chemically modified cytochromes *c*.

A. Freely Diffusing Complexes

Many workers have studied the rate of electron transfer between inorganic electron donors such as ferrocyanide, $[Fe(CN)_6]^{4-}$, and ferricytochrome *c*.[7] An overall second-order rate constant is readily obtained, but the location of the binding sites and their stability constants are more elusive. Our NMR studies indicate that there are

at least six binding sites for $[Fe(CN)_6]^{3-}$ on cytochrome *c*; thus the observed second-order rate constant should be expressed as follows:

$$k_{obs} = \sum_{i}^{6} k_i K_i \tag{16}$$

where k_{obs} is the observed rate, K_i is the association constant for each of the six, presumed-independent binding sites, and k_i is the electron-transfer rate when the donor/acceptor is bound to the protein and whose activation energy may be estimated from Marcus theory.[3,4] At present insufficient data are available to determine the rate and equilibrium constants at each site. Until these parameters are resolved we can make no further fundamental analysis of the rate data. This conclusion applies not only to the reactions of cytochrome *c* with $[Fe(CN)_6]^{n-}$ but also to those with $[Fe(edta)(H_2O)]^{m-}$ and its derivatives. Elsewhere[57] we have indicated that, when the complex may exist in a number of protonation states, it is essential to know which species are undergoing electron exchange and whether or not a proton-transfer step is coupled to the electron-transfer reaction.

Chemical modifications of the surface of cytochrome *c* have been used to study its interaction with a wide range of small molecules and other proteins.[7,49,58–60] These experiments include modification of the positively charged lysine residues of cytochrome *c*, producing neutral or negatively charged derivatives, followed by measurements of the association constants or second-order rates of electron transfer between the derivative and its chosen partner. The variation in the measured rate constants on modification of a specific lysine residue reflects the electrostatic contribution of that lysine to the stability of the reactive complex and is used to delimit the surface of cytochrome *c* through which electron transfer takes place.

Using this method only the free-energy difference between the separated reactants and the reactive complex is measured. So far all analyses of such data have made the assumption that the chemical modification affects only the free energy of the reactive complex and does not change the free energy of the separated reactants. However we have seen that structural changes in cytochrome *c* may be highly cooperative and extend throughout the protein; thus the validity of this assumption is not assured.

There is a peculiarity in the data in that even the most effective modification of a single lysine, e.g., Lys72, which is supposed to be

a required site of binding for anionic reagents, only alters the second-order rate constant by a factor of five.[59] It appears to be essential to have proteins modified in more than one site so as to understand the site specificity and relevance to electron transfer.

B. Covalently Bound Complexes

These experiments make use of electron-transfer reagents which have been covalently bound to the protein surface paralleling the approach of Taube[61] in his analysis of small-molecule electron transfer. The aim of these experiments is to avoid the associative step of reaction complex formation and to avoid ambiguity in the position of the binding site. So far the only complex obtained has the $[Ru(NH_3)_5]^{3+}$ moeity bound to His33 of cytochrome *c*.[62] While the first aim, that of tight binding, is achieved it should be pointed out that His33 is a relatively mobile surface residue and the exact Ru–Fe distance is not known and may not be fixed. Also, particular dynamic states of the protein that affect the haem are coupled to His33 (Section 5F). A second problem is that the site of attachment is relatively far from the iron (15 ± 2 Å). The electron-transfer rate constant here is very slow[63,64] which increases the range of vibrational modes and conformational states of the protein which can take part in activation. Thus it is not clear that the activation parameters of this reaction have any relevence to the physiological reactions of cytochrome *c*. Finally there is controversy in the literature over both the data and its interpretation.[63,64] One interesting feature of the reaction is that the rate constant shows little variation with temperature in the range 0 to 60 °C and remains small even above 60 °C when the Fe(III)–Met80 bond begins to break.[39] This suggests that either the reaction is unactivated or that the temperature dependences of two different processes, perhaps activation of the protein and movement of $[Ru(NH_3)_5]^{3+}$ on the protein surface, oppose each other over this range.

8. CONCLUSIONS

We are now at the final stages of our study of the electron-transfer function of cytochrome *c* in the sense that we know the pieces of information which are not yet available. They are related to each of the steps of reaction.

(1) *Binding.* The structure of the surface of cytochrome *c* is not fixed. We need better ways of describing the surface, perhaps in terms of potential-energy wells, and we need to determine the structures of reactive complexes.

(2) *Internal Structure and Mobility.* We now have a good description of the protein but to relate this description to function we need comparative data relating proteins of different sequence. We also need to know the energetics of the various conformation changes.

(3) *Electron-Transfer Rate.* The rate cannot be said to be understood, or even thoroughly described, in any one case. Only when we have a number of examples of rate constants for this first-order process will we have a chance of resolving the terms which contribute, e.g., the nature of the required motions, and the dependence on distance and the medium.

In the light of the above comments we have to state that recent work has served to show how the physical chemistry of protein-mediated electron transfer may be investigated but that nearly all the fundamental questions for electron transfer within a protein matrix have not yet been answered. This contrasts with the situation in biological photo-induced electron transfer[65,66] but is not too different from that of electron transfer between small molecules in free solution.

Acknowledgments

This work was supported by the Science and Engineering Council (SERC) and the Medical Research Council (MRC). G.R.M. acknowledges the award of an SERC Advanced Fellowship and G.W. thanks the MRC for a Training Fellowship. This is a contribution from the Oxford Enzyme Group.

GLYN WILLIAMS, GEOFFREY R. MOORE
and ROBERT J. P. WILLIAMS

Inorganic Chemistry Laboratory,
University of Oxford,
South Parks Road,
Oxford OX1 3QR, United Kingdom

References

1. G. R. Moore, Z.-X. Huang, C. G. S. Eley, H. A. Barker, G. Williams, M. N. Robinson, and R. J. P. Williams, Faraday Discuss. Chem. Soc. **74**, 311–329 (1982).
2. G. R. Moore and R. J. P. Williams, Coord. Chem. Rev. **18**, 125–197 (1976).

3. R. A. Marcus, Ann. Rev. Phys. Chem. **15**, 155–196 (1964).
4. R. A. Marcus and N. Sutin, Inorg. Chem. **14**, 213–216 (1975).
5. "Electron Transfer Reactions", Faraday Discuss. Chem. Soc. **74** (1982).
6. S. Wherland and H. B. Gray, in *Biological Aspects of Inorganic Chemistry* (A. W. Addison, W. R. Cullen, D. Dolphin, and B. R. James, ed.) (Wiley, New York, 1977), pp. 289–368.
7. G. R. Moore, C. G. S. Eley, and G. Williams, Adv. Inorg. Bioinorg. Mech. **3**, 1–96 (1984).
8. "Mobility and function in proteins and nucleic acids", CIBA Foundation Symp. 93 (1983).
9. R. E. Dickerson, T. Takano, D. Eisenberg, O. B. Kallai, L. Samson, A. Cooper, and E. Margoliash, J. Biol. Chem. **246**, 1511–1535 (1971).
10. T. Tanaka, T. Yamane, T. Tsukihara, T. Ashida, and M. Kakudo, J. Biochem. **77**, 147–162 (1975).
11. Y. Matsuura, Y. Hata, T. Yamaguchi, N. Tanaka, and M. Kakudo, J. Biochem. **85**, 729–737 (1979).
12. T. Takano and R. E. Dickerson, J. Mol. Biol. **153**, 79–115 (1981).
13. H. Ochi, Y. Hata, N. Tanaka, M. Kakudo, T. Sakurai, S. Aihara, and Y. Morita, J. Mol. Biol. **166**, 407–418 (1983).
14. R. E. Dickerson, M. L. Kopka, C. L. Borders, Jr., J. Varnum, J. E. Weinzierl, and E. Margoliash, J. Mol. Biol. **29**, 77–95 (1967).
15. T. Takano, A. Sugihara, O. Ando, T. Ashida, M. Kakudo, T. Horio, Y. Sasada, and K. Okunuki, J. Biochem. **63**, 808–810 (1968).
16. T. Ashida, T. Ueki, T. Tsukihara, A. Sugihara, T. Takano, and M. Kakudo, J. Biochem. **70**, 913–924 (1971).
17. R. E. Dickerson and R. Timkovich, in *The Enzymes*, Vol. 11 (P. Boyer, ed), 3rd ed. (Academic Press, New York, 1975), pp. 397–547.
18. E. Stellwagen, Nature **275**, 73–74 (1978).
19. K. Wuthrich, *N.m.r. in Biological Research: Peptides and Proteins* (Elsevier, Amsterdan, 1976).
20. W. Horrocks, W. De, Jr., and S. Greenberg, Biochim. Biophys. Acta **322**, 38–44 (1973).
21. G. R. Moore, R. J. P. Williams, J. C. W. Chien, L. C. Dickinson, J. Inorg. Biochem. **12**, 1–15 (1980).
22. G. Williams, G. R. Moore, R. Porteous, M. N. Robinson, N. Soffe, and R. J. P. Williams, J. Mol. Biol. (submitted).
23. G. R. Moore, M. N. Robinson, G. Williams, and R. J. P. Williams, J. Mol. Biol. (submitted).
24. J. Boyd, G. R. Moore, and G. Williams, J. Magn. Reson. **58**, 511–516 (1984).
25. C. Mailer and C. P. S. Taylor, Canad. J. Biochem. **85**, 1048–1055 (1972).
26. G. Williams, N. J. Clayden, G. R. Moore, and R. J. P. Williams, J. Mol. Biol. (submitted).
27. A. Kalk and H. J. C. Berendson, J. Magn. Reson. **24**, 343–366 (1976).
28. M. Karplus, J. Am. Chem. Soc. **85**, 2870–2871 (1963).
29. V. F. Bystrov, Prog. Nucl. Magn. Reson. Spectrosc. **10**, 41–81 (1976).
30. K. D. Kopple, G. R. Wiley, and R. Tauke, Biopolymers **12**, 627–636 (1973).
31. M. Delepierre, C. M. Dobson, and F. M. Poulsen, Biochemistry **21**, 4756–4761 (1982).
32. T. N. Bhat, V. Sasisekhran, and M. Vijayan, Int. J. Pept. Protein Res. **13**, 170–184 (1979).
33. B. Dezube, C. M. Dobson, and C. E. Teague, J. Chem. Soc. Perkin Trans. **4**, 730–735 (1981).

34. B. R. Gelin and M. Karplus, Biochemistry **18**, 1256–1268 (1979).
35. S. C. Tam and R. J. P. Williams, Struct. Bonding (submitted).
36. R. J. P. Williams and G. R. Moore, Trends Biochem. Sci. (submitted).
37. R. J. P. Williams, G. R. Moore, and G. Williams, *Prog. Bioorg. Chem. Mol. Biol.* (Y. A. Ovchinikov, ed) (Elsevier, Amsterdam, 1984), pp. 31–39.
38. G. R. Moore, FEBS Lett. **161**, 171–175 (1983).
39. J. Ångstrom, G. R. Moore, and R. J. P. Williams, Biochim. Biophys. Acta. **703**, 87–94 (1982).
40. A. P. Boswell, G. R. Moore, R. J. P. Williams, C. J. A. Wallace, P. J. Boon, R. J. F. Nivard, and G. I. Tesser, Biochem. J. **193**, 493–502 1981).
41. T. Takano and R. E. Dickerson, in *Electron Transport and Oxygen Utilization* (C. Ho, ed) (Elsevier, Amsterdam, 1982), pp. 17–26.
42. S. H. Northrup, M. R. Pear, J. A. McCammon, and M. Karplus, Nature **286**, 304–305 (1980).
43. *Tunneling in Biological Systems* (B. Chance, D. C. DeVault, H. Frauenfelder, R. A. Marcus, J. R. Schrieffer, and N. Sutin, eds.) (Academic Press, New York, 1979).
44. G. R. Moore and R. J. P. Williams, Eur. J. Biochem. **103**, 513–521 (1980).
45. C. G. S. Eley, G. R. Moore, R. J. P. Williams, W. Neupert, P. J. Boon, H. H. K. Brinkhof, R. F. Nivard, and G. I. Tesser, Biochem. J. **205**, 153–165 (1982).
46. P. D. Burns and G. N. La Mar, J. Bio. Chem. **256**, 4934–4939 (1981).
47. M. N. Robinson, A. P. Boswell, Z.-H. Huang, C. G. S. Eley, and G. R. Moore, Biochem. J. **213**, 687–700 (1983).
48. P. Nicholls, Biochim. Biophys. Acta **346**, 261–310 (1974).
49. S. Ferguson-Miller, D. L. Brautigan, and E. Margoliash, in *The Porphyrins* (D. Dolphin, ed.), Vol. VII (Academic Press, New York, 1979), pp. 149–240.
50. B. Chance, C. Saronio, J. S. Leigh, Jr., and A. Waring, in Ref. 43, pp. 483–511.
51. T. L. Poulos and B. C. Finzel, Peptide and Protein Reviews (in press).
52. T. Yonetani, in *The Enzymes* (P. Boyer, ed), 3rd ed., Vol. XIII (Academic Press, New York, 1976), pp. 345–361.
53. R. J. Kassner, J. Am. Chem. Soc. **95**, 2674–2677 (1973).
54. N. K. Rogers, G. R. Moore, and M. J. E. Sternberg, J. Mol. Biol. (in press).
55. Y. Li, K. Leonard, and H. Weiss, Eur. J. Biochem. **116**, 199–205 (1981).
56. L. C. Petersen, FEBS Lett. **94**, 105–108 (1978).
57. G. Williams and G. R. Moore, J. Inorg. Biochem. **22**, 1–10 (1984).
58. E. Margoliash and H. R. Bosshard, Trends Biochem. Sci. **8**, 316–320 (1983).
59. J. Butler, S. K. Chapman, D. M. Davies, A. G. Sykes, S. H. Speck, N. Osheroff, and E. Margoliash, J. Biol. Chem. **258**, 6400–6404 (1983).
60. A. J. Ahmed and F. Millett, J. Biol. Chem. **256**, 1611–1615 (1981).
61. H. Taube, Science **226**, 1028–1036 (1984).
62. K. M. Yocum, J. B. Shelton, J. R. Shelton, W. A. Schroeder, G. Worosila, S. S. Isied, E. Bordingnon, and B. G. Gray, Proc. Natl. Acad. Sci. USA **79**, 7052–7055 (1982).
63. J. Winkler, D. Nocera, K. Yocum, E. Bordignon, and H. B. Gray, J. Am. Chem. Soc. **104**, 5798–5800 (1982).
64. S. S. Isied, C. Kuehn, and G. Worosila, J. Am. Chem. Soc. **106**, 1722–1726 (1984).
65. D. DeVault and B. Chance, Biophys. J. **6**, 825–847 (1966).
66. J. J. Hopfield, Proc. Natl. Acad. Sci. USA **71**, 3640–3644 (1974).